3. C.I.G. Hsu, C.H. Lee, and Y.H. Hsieh, Tri-band bandpass filter with sharp passband skirts designed using tri-section SIRs, IEEE Microwave Wirel Compon Lett 18 (2008), 19–21.
4. F.C. Chen, Q.X. Chu, and Z.H. Tu, Tri-band bandpass filter using stub loaded resonators, Electron Lett 44 (2008), 747–749.
5. X.Y. Zhang, Q. Xue, and B.J. Hu, Planar tri-band bandpass filter with compact size, IEEE Microwave Wirel Compon Lett 20 (2010), 262–264.
6. J.Z. Chen, N. Wang, Y. He, and C.H. Liang, Fourth-order tri-band bandpass filter using square ring loaded resonators, Electron Lett 47 (2011), 858–859.

ON THE ISOLATION OF TWO LTE700/2300/2500 ANTENNAS IN THE LAPTOP COMPUTER

Kin-Lu Wong, Po-Wei Lin, and Tsung-Ju Wu
Department of Electrical Engineering, National Sun Yat-Sen University, Kaohsiung 804, Taiwan, Republic of China;
Corresponding author: wongkl@ema.ee.nsysu.edu.tw

Received 20 September 2012

ABSTRACT: *A simple technique for achieving enhanced isolation between two long-term evolution (LTE)700/2300/2500 antennas for the multiple-input multiple-output operation in the laptop computer is presented. The two antennas are mounted along the top edge of the supporting metal plate, which is generally disposed on the inner surface of the upper cover of the laptop computer. Improved isolation (measured S_{21} better than −30 dB in the LTE700 band and −26 dB in the LTE2300/2500 bands) between the two antennas is easily achieved by adjusting the supporting metal plate to have a length of about 110 mm in the longitudinal direction (orthogonal to the lateral direction or the top-edge direction of the supporting metal plate). Because the length is close to a quarter wavelength of a frequency in the LTE700 band, the excited surface currents in the supporting metal plate will become stronger in the longitudinal direction, which hence causes weaker surface currents flowing along the top edge of the supporting metal plate. This behavior leads to enhanced isolation between the antennas mounted along the top edge of the supporting metal plate. Details of the proposed isolation technique are described, and the obtained results are presented and discussed.* © 2013 Wiley Periodicals, Inc. Microwave Opt Technol Lett 55:1370–1375, 2013; View this article online at wileyonlinelibrary.com. DOI 10.1002/mop.27555

Key words: *mobile antennas; long-term evolution antennas; antenna isolation; multiple-input multiple-output antennas; laptop computer antennas*

1. INTRODUCTION

The long-term evolution (LTE) operation in the multiple-input multiple-output (MIMO) system has recently attracted much attention, mainly because it can provide better mobile broadband and multimedia services than the existing wireless wide area mobile networks and the wireless local area networks. For the LTE MIMO operation, it is important to achieve good isolation between the LTE antennas embedded in the portable communication devices such as the mobile handsets and laptop computers. Some techniques especially suitable for applications in the mobile handsets to achieve enhanced isolation of the LTE antennas in the 700-MHz band have been reported [1–9]. The techniques include using a suspended-line related design between two closely-located antennas [1, 6, 8], or adding a band stop filter at the corner of each one of the two antennas mounted at opposite edges of the system ground plane [2], or using an

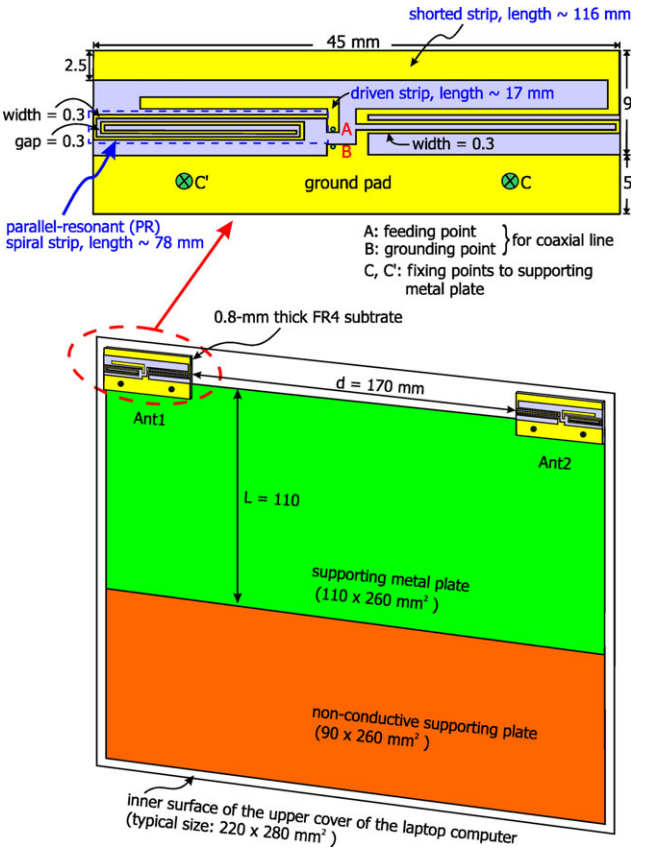

Figure 1 Geometry of two LTE antennas mounted along the top edge of the supporting metal plate, which is generally disposed on the inner surface of the upper cover of the laptop computer. [Color figure can be viewed in the online issue, which is available at wileyonlinelibrary.com]

LC-based branchline hybrid coupler to integrate with the antennas to decouple the ports [3], or using the metamaterial antennas to limit the excited surface currents in the system ground plane to thereby decrease the port coupling [4], or using the monopole antennas with magnetodielectric materials [5], or using two ferrite antennas with a protruded ground plane in-between [7], or using two coupled-fed loop antennas with a protruded ground plane in-between [9], and so on.

For applications in the laptop computers, however, very few isolation techniques have been reported for achieving high-isolation LTE antennas. Note that the environment for the embedded antennas in the laptop computer is quite different from that in the mobile handset. For example, the embedded antennas in the laptop computer are generally connected to the supporting metal plate which is disposed on the inner surface of the upper cover of the laptop computer and usually has a much larger size than the system ground plane of the mobile handset, hence the isolation techniques suitable for mobile handset applications may not be promising to be applied in the laptop computers.

In this article, we propose a simple isolation technique that is easy to be implemented in the laptop computers for the LTE MIMO antennas to achieve high isolation. Two small-size LTE antennas capable of covering the LTE700/2300/2500 bands (704–787/2300–2400/2500–2690 MHz) are to be mounted along the top edge of the supporting metal plate. Owing to the large space along the top edge, which is different from the condition in the mobile handset, the two LTE antennas can be placed, respectively, at the left and right corners of the top edge to achieve a large distance between the antennas. However, it is

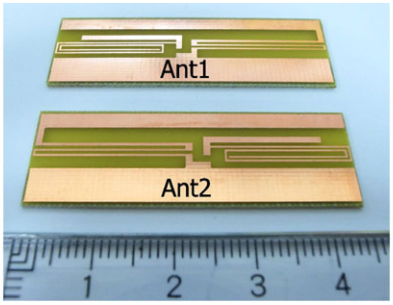

(a)

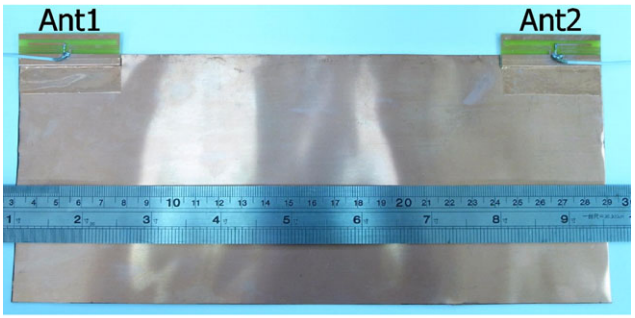

(b)

Figure 2 Photos of (a) the fabricated antennas (Ant1 and Ant2) and (b) the two antennas mounted along the top edge of the supporting metal plate. [Color figure can be viewed in the online issue, which is available at wileyonlinelibrary.com]

usually observed that the surface currents excited in the supporting metal plate are strong along the top edge thereof, which leads to increased coupling between the antennas, especially for the LTE operation in the 700-MHz band. To overcome this problem, it is proposed that the supporting metal plate be selected to have a length of about 110 mm in the longitudinal direction (orthogonal to the lateral direction or the top-edge direction of the supporting metal plate). In this case, stronger excited surface currents in the supporting metal plate can be directed to be in the longitudinal direction, because the path length along the longitudinal direction is close to a quarter-wavelength of a frequency in the LTE700 band and hence can become resonant in the LTE700 band. This behavior will therefore cause weaker surface currents excited along the top edge of the supporting metal plate and lead to enhanced isolation

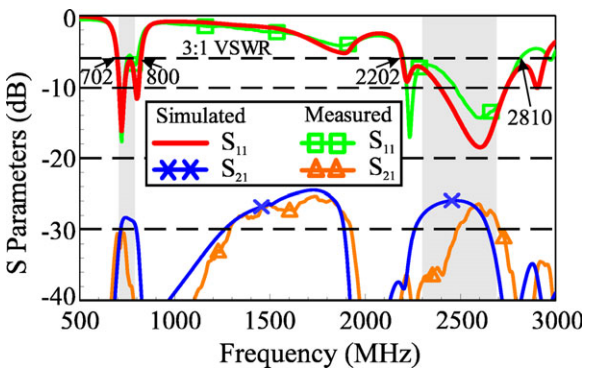

Figure 3 Measured and simulated S parameters (S_{11} and S_{21}) of the two LTE antennas mounted as shown in Figure 2(b). [Color figure can be viewed in the online issue, which is available at wileyonlinelibrary.com]

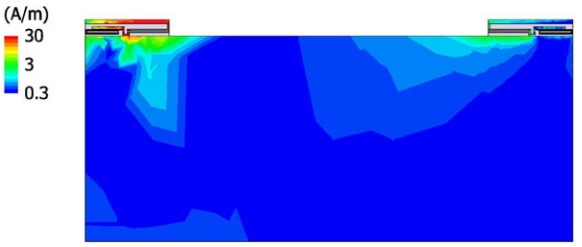

Figure 4 Simulated surface current distributions in the supporting metal plate at 745 MHz for the proposed design studied in Figure 3. [Color figure can be viewed in the online issue, which is available at wileyonlinelibrary.com]

between the two LTE antennas. The proposed isolation technique can provide a measured S_{21} of better than −30 dB in the LTE700 band and −26 dB in the LTE2300/2500 bands between the antennas in this study. Details of the proposed isolation technique are described, and the obtained results using two small-size planar LTE antennas are presented and discussed.

2. PROPOSED ISOLATION TECHNIQUE

Figure 1 shows the geometry of two LTE antennas (Ant1 and Ant2) mounted along the top edge of the supporting metal plate disposed on the inner surface of the upper cover of the laptop computer. Note that a laptop computer equipped with a 13-inch display panel is studied. In this case, it is reasonable that the size of the inner surface of the upper cover of the laptop computer is selected to be about 200 × 260 mm^2. To provide enough supporting strength as that of a complete supporting metal plate for the upper cover, a nonconductive supporting plate (e.g., a reinforced plastic slab) of size 90 × 260 mm^2 can be added to combine with the proposed metal plate of length L selected to be 110 mm, which is close to a quarter wavelength of a frequency in the LTE700 band (704–787 MHz). With the proposed structure of the supporting plate which comprises the metal plate of size 110 × 260 mm^2 and the nonconductive supporting plate of size 90 × 260 mm^2, enough supporting strength for the upper cover can be obtained and enhanced isolation between the two LTE antennas in the LTE700/2300/2500 bands can be achieved as well.

As shown in the figure, the two LTE antennas of Ant1 and Ant2 are of the same configuration and are mounted, respectively, at the left and right corners of the top edge of the metal plate. The size of the antennas above the top edge is 9 × 45 mm^2 only, and the distance d between the two antennas is 170 mm. The antennas have a planar structure and can be fabricated at low cost by printing on a 0.8-mm thick FR4 substrate of relative permittivity 4.4 and loss tangent 0.024. Note that the ground pad portion is to be connected to the metal plate via two fixing points C, C′ in this study. Also, owing to the planar structure with a thin profile, the proposed antenna is very suitable for applications in the ultrabook computers which are generally with a very slim profile.

The antenna is composed of a driven strip, a shorted strip and a parallel-resonance (PR) spiral strip. The driven strip has a length of about 17 mm and can contribute a resonant mode at about 2.5 GHz to cover the LTE2300/2500 bands. The shorted strip has a length of about 116 mm, which is close to a quarter wavelength of a frequency in the LTE700 band. Note that the shorted strip has a long narrow section of width 0.3 mm close to its shorted end to the ground pad. The long narrow section functions like a printed distributed inductor [10–12] to

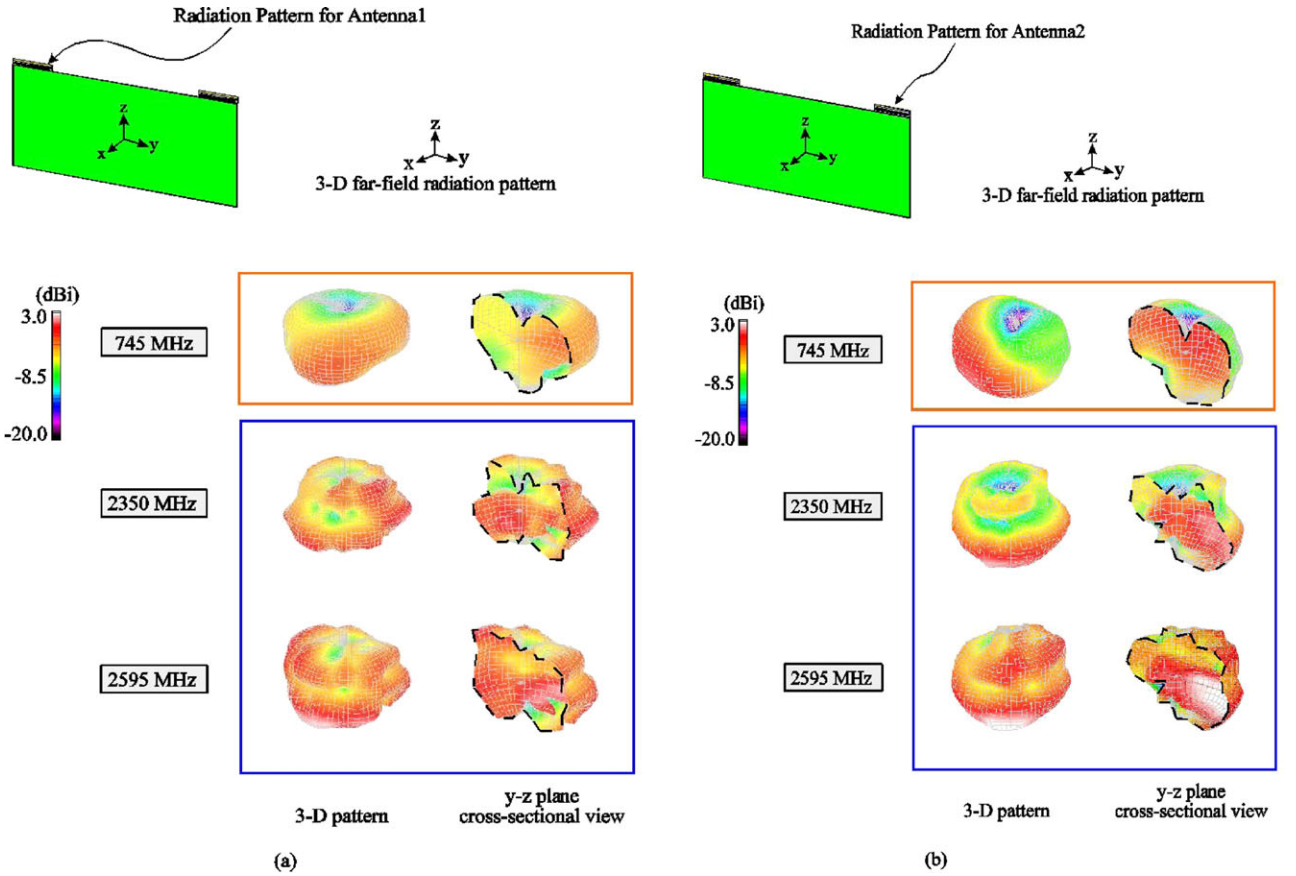

Figure 5 Measured 3D total-power radiation patterns for Antenna 1 and 2 at 745, 2350, and 2595 MHz for the proposed design studied in Figure 3. (a) Antenna 1 (Ant1). (b) Antenna 2 (Ant2). [Color figure can be viewed in the online issue, which is available at wileyonlinelibrary.com]

effectively help shift the excited resonant mode to lower frequencies. The shorted strip can contribute a resonant mode at about 700 MHz with a compact size. However, the bandwidth of the resonant mode cannot cover that required for the LTE700 band. With the aid of the spiral strip of length 78 mm, a PR can occur at a frequency higher than the desired LTE700 band, which can then lead to the generation of a new resonance (zero reactance) inside the desired LTE700 band. The new resonance results in a new resonant mode occurred at about 800 MHz to combine with the original resonant mode at about 700 MHz to form a wide operating band to cover the LTE700 band. The operating principle of using an excited parallel resonance to create a new resonant mode for bandwidth enhancement has been studied in Refs. 13–17.

As for the enhanced isolation between the two LTE antennas, it is obtained by decreasing the excited surface currents flowing along the top edge of the metal plate, which in turn results in decreased coupling between the two LTE antennas. This is easily achieved in the proposed design, because the metal plate in the longitudinal direction will become resonant in the LTE700 band. In this case, stronger excited surface currents flowing in the longitudinal direction can be expected. This can lead to weaker surface currents flowing along the top edge of the metal plate, and hence enhanced isolation between the two antennas can be obtained. The obtained S_{21} in the LTE700 band can be improved by about 15 dB, from worse than -15 dB to about -30 dB. Also, for operating in the LTE2300/2500 bands, because the two antennas have a large distance in-between, good isolation (S_{21} better than -25 dB) can also be obtained in the LTE2300/2500 bands. That is, good isolation in the LTE700/2300/2500 bands can be achieved for the two LTE antennas in the proposed design.

3. RESULTS OF PROPOSED DESIGN

The proposed LTE antennas have been fabricated, and the photos of the fabricated antennas mounted along the top edge of the supporting metal plate are shown in Figure 2. Note that the nonconductive supporting plate shown in Figure 1 is not included in the study, and it is expected that there will be generally no differences in the obtained results for the cases with and without the nonconductive supporting plate such as a reinforced plastic slab. Also, in the experiment, Ant1 and Ant2 are, respectively, connected to a 50-Ω coaxial line, with its central conductor and outer grounding sheath connected to point A (the feeding point) and point B (the grounding point), respectively.

Figure 3 shows the measured and simulated S parameters of the two LTE antennas mounted as shown in Figure 1. The simulated results are obtained using the three-dimensional (3D) full-wave electromagnetic field simulator HFSS version 14 [18]. Good agreement between the measurement and simulation is seen. Because the antennas are of the same dimensions and symmetrically disposed at opposite corners of the top edges, the S_{11} and S_{22} versus frequencies are generally the same. The S_{22} curve is hence not shown in the figure for brevity. Both Ant1 and Ant2 cover the LTE700 band in the lower band and the LTE2300/2500 bands in the upper bands. As described in Section 2, the first and second resonant modes in the lower band are generated owing to the shorted strip and the PR spiral strip,

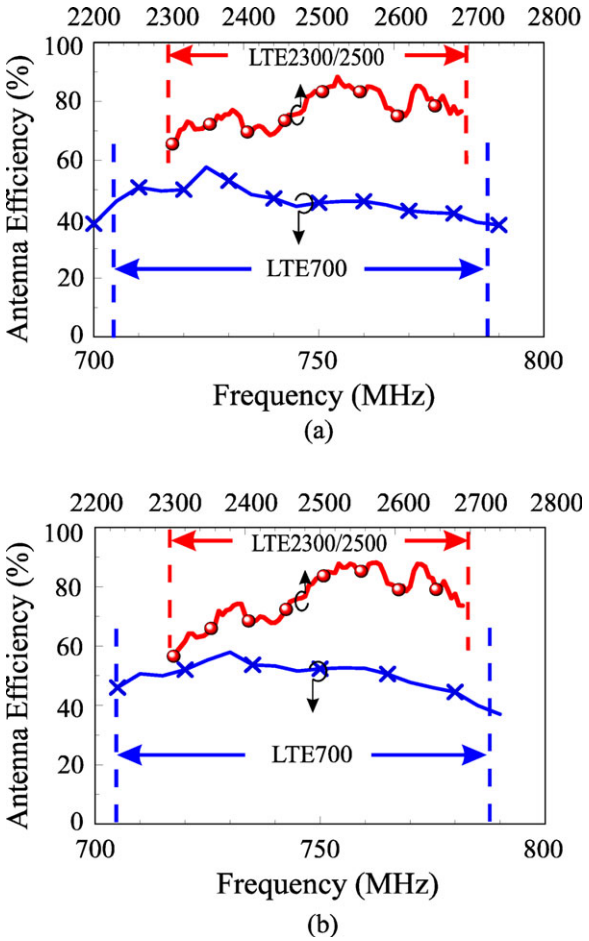

Figure 6 Measured antenna efficiency (mismatching loss included) of the two LTE antennas studied in Figure 3. (a) Antenna 1 (Ant1). (b) Antenna 2 (Ant2). [Color figure can be viewed in the online issue, which is available at wileyonlinelibrary.com]

respectively, and the resonant mode in the upper band is contributed by the driven strip. In the desired operating bands, the impedance matching is better than 3:1 VSWR (6-dB return loss), which is widely used as the design specification of the internal mobile device antennas. The measured S_{21} between Ant1 and Ant2 is seen to be better than -30 dB in the LTE700 band and better than -26 dB in the LTE2300/2500 bands.

Figure 4 shows the simulated surface current distributions in the supporting metal plate at 745 MHz for the proposed design studied in Figure 3. The results are obtained with Ant1 excited. Stronger excited surface currents in the longitudinal direction are seen for the metal plate portion near Ant1 (compared to the corresponding results shown in Fig. 9), which causes weaker surface currents flowing along the top edge of the metal plate and leads to decreased coupling between Ant1 and Ant2. More results about the excited surface currents for different lengths (L) of the supporting metal plate are presented and discussed in Figure 9.

Figure 5 shows the measured 3D total-power radiation patterns for Ant1 and Ant2 at 745, 2350, and 2595 MHz for the proposed design studied in Figure 3. At 745 MHz, the radiation patterns of Ant1 are stronger in the $+y$ direction, whereas Ant2 shows stronger radiation in the $-y$ direction. This is largely owing to the excited surface currents flowing along the top edge in the different directions for Ant1 and Ant2 (the currents flowing in the $+y$ direction for Ant1 and in the $-y$ direction for Ant2). At higher frequencies (2350 and 2595 MHz), more variations are seen in the radiation patterns for Ant1 and Ant2, which is owing to the much smaller wavelengths at 2350 and 2595 MHz compared to that at 745 MHz in the LTE2300/2500 bands.

Figure 6 shows the measured antenna efficiency of the two LTE antennas studied in Figure 3. The antenna efficiency includes the mismatching losses. Similar antenna efficiencies for Ant1 and Ant2 are seen, with small discrepancies which may be owing to some small fabrication errors or small differences in the measurement alignments of the two antennas. For the LTE700 band, although the antenna size (9×45 mm^2 or about $0.02\lambda \times 0.1\lambda$) is very small (compared to the operating wavelengths in the LTE700 band, the radiation efficiencies of the Ant1 and Ant2 are better than about 40%. Although for the LTE2300/2500 bands, the radiation efficiency of the Ant1 and Ant2 are better than about 60%. The obtained antenna efficiencies are acceptable for practical applications.

Effects of the distance d between the two LTE antennas on the S parameters are also analyzed. Results for the distance $d =$ 60 and 100 mm are presented in Figure 7. In Figure 7, Ant1 is fixed at the left corner, whereas Ant2 is moved to be closer to Ant1 to vary the distance in-between. Note that the case in Figure 1 is with a distance d of 170 mm. By comparing the simulated results shown in Figure 3, the S_{21} in the LTE700 band is quickly degraded from about -28 dB for $d = 170$ mm to -16

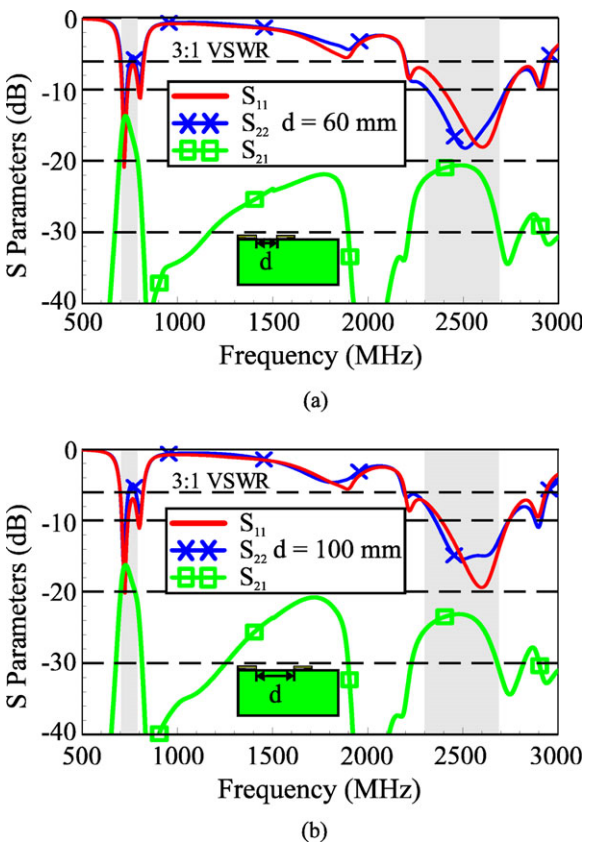

Figure 7 Simulated S parameters of the two LTE antennas with different distances in-between. (a) $d = 60$ mm. (b) $d = 100$ mm. Antenna 1 is fixed at the left corner, with Antenna 2 shifted toward Antenna 1. [Color figure can be viewed in the online issue, which is available at wileyonlinelibrary.com]

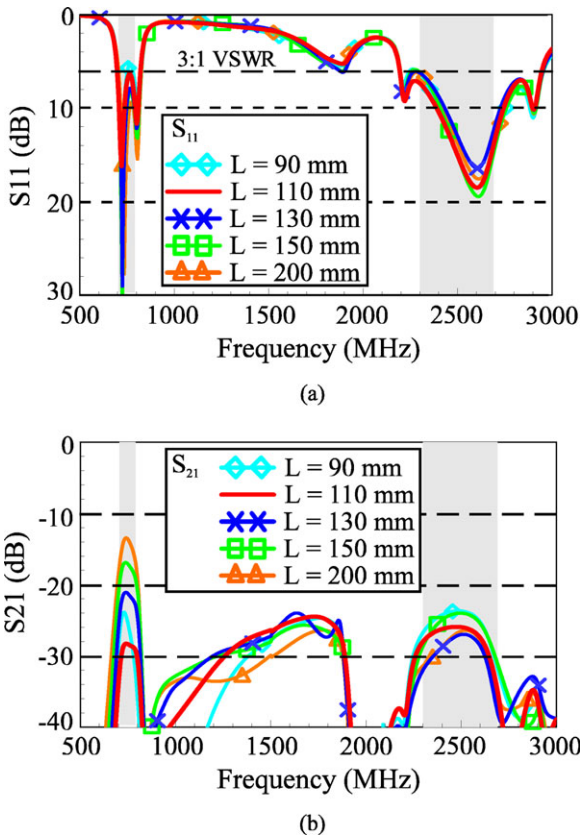

Figure 8 Simulated S parameters of the two LTE antennas as a function of the length L of the supporting metal plate. (a) S_{11}. (b) S_{21}. [Color figure can be viewed in the online issue, which is available at wileyonlinelibrary.com]

dB for $d = 100$ mm and to -13.8 dB for $d = 60$ mm. In the LTE2300/2500 bands, the S_{21} is also degraded from about -26 dB for $d = 170$ mm to -24 dB for $d = 100$ mm and to -20.2 dB for $d = 60$ mm. The results show that the distance d greatly affects the isolation between Ant1 and Ant2, especially in the LTE700 band. Also note that the two antennas are of the same dimensions as studied in Figure 3, and the S_{11} and S_{22} show that the impedance matching of the two antennas are slightly affected by the distance d.

Effects of the length L of the supporting metal plate on the S parameters are also studied. The S_{11} results for the length L varied from 90 to 200 mm are shown in Figure 8(a), whereas the S_{21} results are presented in Figure 8(b). Note that, in this case, the simulated results of the S_{22} are the same as those of the S_{11} and are not shown for brevity. It is first seen that the S_{11} is slightly affected by the variations in the length L. The S_{21}, however, is greatly affected by the variations in the length L. In the LTE700 band, the S_{21} is varied from about -13.8 to -28 dB when the length L is varied from 90 to 200 mm. The case with $L = 200$ mm shows the worst S_{21} ($= -13.8$ dB). This behavior can be explained more clearly from the simulated surface current distributions in the supporting metal plate with the length $L = 130$, 150, and 200 mm shown in Figure 9. In this study, the Ant1 is excited. For $L = 200$ mm, the strongest excited surface currents in the horizontal direction (parallel to the top edge of the metal plate) are observed. This leads to strong coupling between the two antennas, resulting in a large S_{21} of -13.8 dB (about 15 dB larger than that for $L = 110$ mm). Although for the S_{21} in the LTE2300/2500 bands, the variations are much smaller (from about -24 to -27.5 dB). The results suggest that when the two LTE antennas have a larger distance in-between, better S_{21} can be easily obtained for higher frequencies (LTE2300/2500 bands). However, for lower frequencies (LTE700 band), better S_{21} cannot be obtained if the length L of the supporting metal plate is not properly selected.

4. CONCLUSION

It has been demonstrated that two LTE/700/2300/2500 laptop computer antennas mounted at opposite corners of the top edge of the supporting metal plate therein can have much enhanced isolation simply by selecting a proper longitudinal length of the supporting metal plate. When the length orthogonal to the lateral or top-edge direction is chosen to be about a quarter wavelength of a frequency in the LTE700 band, the excited surface currents in the longitudinal direction of the supporting metal plate have been observed to be stronger. This in turn leads to weaker

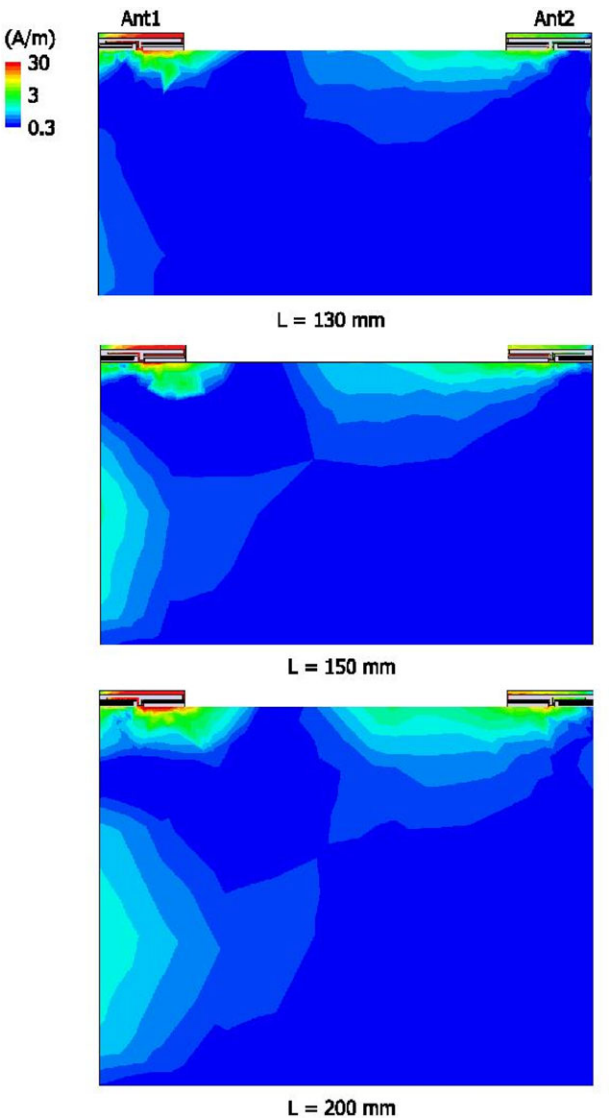

Figure 9 Simulated surface current distributions in the supporting metal plate with the length $L = 130$, 150, and 200 mm at 745 MHz. Other parameters are the same as in Figure 8. [Color figure can be viewed in the online issue, which is available at wileyonlinelibrary.com]

excited surface currents flowing along the top edge of the supporting metal plate, and hence enhanced isolation between the two LTE antennas has been obtained. The measured S_{21} in the LTE700 and LTE2300/2500 bands has been observed to be better than −30 dB and −26 dB, respectively. Good radiation characteristics of the two LTE antennas have also been obtained. The proposed isolation technique for LTE antennas is promising to be applied in practical laptop computers.

REFERENCES

1. G. Park, M. Kim, T. Yang, J. Byun, and A.S. Kim, The compact quad-band mobile handset antenna for the LTE700 MIMO application, IEEE Antennas Propagat Soc Int Symp, Charleston, SC, 2009.
2. M.S. Han and J. Choi, Multiband MIMO antenna with a band stop filter for high isolation characteristics, IEEE Antennas Propagat Soc Int Symp, Charleston, SC, 2009.
3. R.A. Bhatti, S. Yi, and S.O. Park, Compact antenna array with port decoupling for LTE-standardized mobile phones, IEEE Antennas Wirel Propag Lett 8 (2009), 1430–1433.
4. N. Lopez, C. Lee, A. Gummalla, and M. Achour, Compact metamaterial antenna array for long term evolution (LTE) handset application, IEEE International Workshop on Antenna Technology (iWAT), Santa Monica, CA, 2009, pp. 1–4.
5. Y.S. Shin and S.O. Park, A monopole antenna with a magneto-dielectric material and its MIMO application for 700 MHz-LTE-band, Microwave Opt Technol Lett 52 (2010), 2364–2367.
6. H. Bae, F.J. Harackiewicz, M.J. Park, T. Kim, N. Kim, D. Kim, and B. Lee, Compact mobile handset MIMO antenna for LTE700 applications, Microwave Opt Technol Lett 52 (2010), 2419–2422.
7. J. Lee, Y.K. Hong, S. Bae, G.S. Abo, W.M. Seong, and G.H. Kim, Miniature long-term evolution (LTE) MIMO ferrite antenna, IEEE Antennas Wirel Propag Lett 10 (2011), 603–606.
8. A. Tatomirescu, M. Pelosi, M.B. Knudsen, O. Franek, and G.F. Pedersen, Port isolation method for MIMO antenna in small terminals for next generation mobile networks, IEEE Vehicular Technology Conf (VTC fall), San Francisco, CA, 2011, pp. 1–5.
9. K.L. Wong, T.W. Kang, and M.F. Tu, Antenna array for LTE/WWAN and LTE MIMO operations in the mobile phone, Microwave Opt Technol Lett 53 (2011), 1569–1573.
10. C.H. Chang and K.L. Wong, Small-size printed monopole with a printed distributed inductor for penta-band WWAN mobile phone application, Microwave Opt Technol Lett 51 (2009), 2903–2908.
11. K.L. Wong, W.J. Wei, and L.C. Chou, WWAN/LTE printed loop antenna for tablet computer and its body SAR analysis, Microwave Opt Technol Lett 53 (2011), 2912–1919.
12. K.L. Wong and S.C. Chen, Printed single-strip monopole using a chip inductor for penta-band WWAN operation in the mobile phone, IEEE Trans Antennas Propag 58 (2010), 1011–1014.
13. Y.W. Chi and K.L. Wong, Very-small-size folded loop antenna with a band-stop matching circuit for WWAN operation in the mobile phone, Microwave Opt Technol Lett 51 (2009), 808–814.
14. K.L. Wong and T.J. Wu, Small planar internal WWAN tablet computer antenna, Microwave Opt Technol Lett 54 (2012), 426–431.
15. K.L. Wong, Y.W. Chang, and S.C. Chen, Bandwidth enhancement of small-size WWAN tablet computer antenna using a parallel-resonant spiral slit, IEEE Trans Antennas Propag 60 (2012), 1705–1711.
16. K.L. Wong and P.J. Ma, Small-size WWAN monopole slot antenna with dual-band band-stop matching circuit for tablet computer application, Microwave Opt Technol Lett 54 (2012), 875–879.
17. K.L. Wong and Y.C. Liu, Small-size WWAN tablet computer antenna with distributed and lumped parallel resonant circuits, Microwave Opt Technol Lett 54 (2012), 1348–1353.
18. ANSYS HFSS. Ansoft Corp., Pittsburgh, PA. Available at http://www.ansys.com/products/hf/hfss/

THE ON-LINE MEASUREMENT OF DIMETHOATE SOLUTION'S DEGRADATION BASED ON A LONG-PERIOD GRATING

Xingliu Hu,[1] Dakai Liang,[2] Ting Fang,[1] Yan Wang,[1] and Dan Li[1]
[1] College of Information and Electric Engineering, Anhui University of Technology, Ma'an shan, Anhui 243032, China; Corresponding author: xinghu8@163.com
[2] The Aeronautical Science Key Laboratory for Smart Material and Structures, Nanjing University of Aeronautics and Astronautics, Jiangshu, Nanjing 210016, China

Received 20 September 2012

ABSTRACT: *A long-period grating is used to detect the degradation of dimethoate solutions which is achieved by the electrocoagulation technology combined with ultrasonic waves in this article. This fiber-based device can indicate the concentration of dimethoate solutions instantaneously without being sampled. It can be applied in the chemistry industry for process control.* © 2013 Wiley Periodicals, Inc. Microwave Opt Technol Lett 55:1375–1379, 2013; View this article online at wileyonlinelibrary.com. DOI 10.1002/mop.27554

Key words: *fibre optic sensors; long-period fiber grating; refractive index; concentration measurements; coupled mode theory*

1. INTRODUCTION

Dimethoate, a widely used organophosphate pesticide present in natural waters (ground and surface water), has some features, such as high chemical oxygen demand (COD) value, high content of organic phosphorus, toxicity, and poor biodegradability. It has become a major unavoidable threat for the life of human beings and useful microorganisms. How to reduce and eliminate the contamination of dimethoate becomes an increasingly urgent task. An important index of evaluating the degradation of dimethoate solution is the concentration of it. The detection method of dimethoate concentration has the vital significance to the degradation process. Various sensing techniques have been reported for measuring dimethoate concentration, for example, thin-layer chromatography and bromating method [1], liquid chromatography [2] and gas chromatography [3], and so forth.

These methods are reliable and can accurately measure the concentration. However, such schemes are somewhat complex and lack the ability to do on-line detection of the solutions concentration. A great deal of time has taken to collect the dimethoate samples and to carry out the concentration test. This process used for sampling and testing is not congruous with dimethoate degradation, which is a continuous process. All these methods are also not suitable to rapid measurement of large scale.

There is an increasing interest of the governments and industries in the development of methods and equipments to be used in the environment control. Optical fiber sensors from applications standpoint present many interesting characteristics, such as small volume, reduced weight, immunity to electromagnetic interference, low insertion losses, high sensitivity, fast response, spectral multiplexing, low back reflection, high network compatibility, and so forth. These properties make the optical fiber sensors safe and suitable to on-line measurements.

The long-period grating (LPG) sensors are capable of responding to refractive index change immediately [4]. They are thus appropriate for continuous real-time monitoring. They can detect the concentration value without the need for handling the